



New triphenylamine-based poly(amine-imide)s with carbazole-substituents for electrochromic applications

Yu Liu^{a,*}, Danming Chao^b, Hongyan Yao^b

^a Institute of Metal Research Chinese Academy of Sciences, Shenyang 110016, China

^b Alan G. MacDiarmid Lab College of Chemistry, Jilin University, Changchun 130023, China

ARTICLE INFO

Article history:

Received 25 February 2014

Received in revised form 9 April 2014

Accepted 11 April 2014

Available online 24 April 2014

Keywords:

Poly(amide-imide)

Synthesis

Electrochromic properties

Triphenylamine

Carbazole

ABSTRACT

A new carbazole-derived triphenylamine-containing diimide-diacid monomer (5), 4,4'-bis(trimellitimidido)-4''-N-carbazolytriphenylamine, is prepared by the condensation of 4,4'-diamino-4''-N-carbazolytriphenylamine (4) and two molar equivalents of trimellitic anhydride (TMA). A series of new poly(amide-imide)s (PAIs) 7a–7d with carbazole-substituted triphenylamine units are prepared by direct polymerization from the new diimide-diacid (5) and various aromatic diamines (6a–6d). The PAIs shows high glass transition temperature between 269 and 297 °C, and high 5% weight loss temperature between 526 and 561 °C under nitrogen environment. Cyclic voltammograms of the PAIs films, which are casted onto the indium–tin oxide (ITO)-coated glass substrate, exhibit two reversible oxidation redox couples at 1.05–1.08 V and 1.38–1.46 V under an anodic sweep. The PAI-7a film reveals excellent stability of electrochromic characteristics for the radical cations generated, changing color from original pale yellowish neutral form to the green and then to dark blue oxidized forms. Furthermore, the anodically coloring of PAI-7a shows high coloration efficiency (CE = 205 cm²/C), high contrast of optical transmittance change ($\Delta T = 80\%$ at 776 nm) and long-term redox reversibility.

© 2014 Elsevier B.V. All rights reserved.

1. Introduction

Electrochromic materials, comprised redox-active species, exhibit significant, lasting, and reversible changes in color upon reduction or oxidation [1]. Color changes are commonly between a transparent state, where the chromophore only absorbs in the UV region, and a colored state, or between two colored states in a given electrolyte solution. The potential applications of electrochromic materials include optical switching devices, automatic anti-glazing mirrors, smart windows, large-area information panels, electronic papers and chameleon materials

[2–9]. The properties of electrochromism are found not only in conducting polymers, but also in variety of organic and inorganic materials. The uses of conjugated polymers as active layers in electrochromic devices become popular because of the outstanding electrochromic properties such as fast switching time, ease of synthesis, and wide range of colors, which can be achieved through simple chemical synthesis [10]. The difficulties in achieving satisfactory values for all these parameters at the same time stimulate the development of new methods of electrochromic films preparation, new materials and new components for the devices [11].

Aromatic polyimides (PIs) are well known as useful high performance materials because of their excellent thermal stability, mechanical, electric and optical properties [12–14]. However, the widespread applications of PIs are often limited by processing difficulties because of their

* Corresponding author. Address: Institute of Metal Research Chinese Academy of Sciences, 72 Wenhua Road, Shenyang 110016, China. Tel./fax: +86 024 83978040.

E-mail address: yliu@imr.ac.cn (Y. Liu).

poor solubility and high processing temperature, which are caused by rigid polymer backbones and the strong inter-chain interaction [15,16]. To overcome these problems, typical approaches include the introduction of flexible linkages, kinked or unsymmetrical structures, bulky packing-disruptive units, and bulky lateral groups into the polymer backbone. In our previous work several soluble fluorinated poly(ether imide)s with different pendant groups have been explored, and the introduction of bulky trifluoromethyl group into polymer backbones result in an enhanced solubility and optical transparency [17]. Another common approach for increasing solubility and processability of PIs without sacrificing high thermal stability is the development of various copolyimides. Replacement of polyimides by copolyimides such as poly(amide-imide)s (PAIs) may be useful in modifying the intractable character of polyimides [18,19]. Because of the PAIs possess both amide and imide groups in their mainchain. This class of polymers combines the advantages of polyamides and polyimides and offers good comprehensive properties such as high thermal property and processability.

In recent years, triarylamine-based PAIs with attractive electrochromic properties have been reported in G.S. Liou's laboratory [20]. Triarylamine derivatives are well-known for their electroactive and photoactive properties, which make them be used as photoconductors, hole-transporters, and light-emitters. Polymers bearing triarylamine units are being received considerable interest as ideal hole-transporters, and light-emitting diodes (OLEDs) because of the strong electron-donating and hole-transporting/injecting properties of triarylamine units [21]. What's more, triarylamine can be easily oxidized to form stable radical cations, and the oxidation process is always associated with a strong change of coloration [22]. Except triarylamine, carbazole is another well-known hole-transporting and light-emitting unit. From structural point of view, carbazole differs from diphenylamine in its planar structure because it can be further imagine as the bonded diphenylamine; the thermal stability of materials with the incorporation of carbazolyl units therefore is improved. In addition, carbazole could be easily functionalized at its 3,6-, 2,7-, or *N*-positions and then covalently linked to polymeric systems, both in the main chain as building blocks and in a side chain as pendant groups [23]. Thus, incorporation of three-dimensional, packing-disruptive triarylamine and carbazole units into the poly(amide-imide) backbone not only enhance the solubility but also form some new electronic factions of poly(amide-imide) such as electrochromic characteristics.

In some reports, the triphenylamine cationic radical of the first electron oxidation is not stable. However, the coupling reactions that afford stable cationic radical are greatly prevented when the phenyl groups are incorporated by electron-donating substituents at the para position of triarylamines [24,25]. In this contribution, we reported the synthesis of novel carbazole-derived triphenylamine-containing aromatic dicarboxylic acid monomer, 4,4'-bis(trimellitimido)-4''-*N*-carbazolytriphenylamine (5), and its derived PAIs bearing electron-rich pendent triphenylamine and carbazole groups. The PAIs exhibited good sol-

ubility and excellent thermal properties. The electrochemical and electrochromic properties of these films prepared by casting the PAIs onto an indium-tin oxide (ITO)-coated glass substrate are also described herein.

1.1. Measurements

IR spectra (KBr) were measured on a Nicolet Impact 410 Fourier transform infrared spectrometer. ¹H NMR and ¹³C NMR were recorded on a Bruker 510 NMR spectrometer (500 MHz) with tetramethyl silane as a reference. Elemental analyses were performed on an Elemental Analyses MOD-1106. Gel permeation chromatograms (GPC) using polystyrene as a standard were obtained on a Waters 410 instrument with a DMF as an eluent at a flow rate of 1 mL/min. Inherent viscosity was determined on an Ubblohe viscometer in thermostatic container with the polymer concentration of 0.5 g/dL in NMP at 30 °C. Differential scanning calorimetry (DSC) measurements were performed on a Mettler Toledo DSC 821^e instrument at a heating rate of 20 °C/min under nitrogen. Thermal gravimetric analyses (TGA) were determined in nitrogen atmosphere using a heating rate of 10 °C/min and polymers were contained within open aluminum pans on a PERKIN ELMER TGA-7. The mechanical tests in tension were carried out using a SHIMADZU AG-I at a constant crosshead speed of 10 mm/min. Wide-angle X-ray diffraction (WAXD) measurements were carried out at room temperature using a Rigaku/max-rA diffractometer equipped with a Cu K α radiation source. Voltammograms were presented with the potential pointing to the left and with increasing anodic currents pointing downwards. Cyclic voltammetry was performed with the use of a three-electrode cell in which ITO (polymer films area about 0.4 cm \times 2.5 cm) was used as a working electrode. A platinum wire was used as an auxiliary electrode. All cell potentials were taken with the use of a homemade Ag/AgCl, KCl (sat.) reference electrode. The spectroelectrochemical cell was composed of a 1 cm cuvette, ITO as a working electrode, a platinum wire as an auxiliary electrode and Ag/AgCl reference electrode. Absorption spectra were measured by a Shimadzu UV 3101-PC spectrophotometer.

2. Experimental

2.1. Materials

All the reagents were purchased from commercial sources and used as received. Carbazole (Acros), 4-fluoronitrobenzene (Acros), trimellitic anhydride (TMA) (TCI), triphenyl phosphite (TCI), 10% palladium on charcoal (Pd/C, TCI), and hydrazine monohydrate (TCI) were used as received. *N,N*-dimethylformamide (DMF), *N*-Methyl-2-pyrrolidone (NMP) and pyridine were purified by distillation under reduced pressure over calcium hydride and stored over 4 Å molecular sieve. 1,4-Bis(4-amino-2-trifluoromethylphenoxy) benzene (6FAPB) was synthesized in our laboratory according to the literature. 4,4'-Oxydianiline (ODA) (TCI) and 1,4-bis(4-aminophenoxy) benzene (APB)

(TCl) were used without further purified. Bu_4NClO_4 was recrystallized from ethyl acetate under nitrogen atmosphere and then dried in vacuum prior to use.

2.2. Monomer synthesis

2.2.1. Synthesis of *N*-(4-nitrophenyl) carbazole (1)

According to the synthesis procedure reported previously [26], compound 1 (mp: 208–210 °C) was prepared by nucleophilic fluoro-displacement reaction of *p*-fluoronitrobenzene with carbazole in the presence of anhydrous potassium carbonate.

IR (KBr): 1580, 1312 cm^{-1} (NO_2 stretch). ^1H NMR (500 MHz, $\text{DMSO}-d_6$, δ , ppm): 7.36 (t, 2H), 7.48 (t, 2H), 7.56 (d, 2H), 7.98 (d, 2H), 8.28 (d, 2H), 8.50 (d, 2H).

2.2.2. Synthesis of *N*-(4-aminophenyl) carbazole (2)

To a refluxed solution of compound 1 (1.44 g, 5.00 mol) and Pd/C (0.0720 g) in ethanol (10 mL) was added dropwise hydrazine monohydrate. The mixture was refluxed for 4 h and cooled to room temperature. Pd/C was removed by filtration through Celite and the filtrate was concentrated to give compound 2 as a clear viscous liquid (1.24 g) in 94 % yield. IR (KBr): 3460, 3379 cm^{-1} (NH_2 stretch). ^1H NMR (500 MHz, $\text{DMSO}-d_6$, δ , ppm): 8.19 (d, 2H), 7.40 (t, 2H), 7.27–7.21 (m, 4H), 7.18 (d, 2H), 6.81 (d, 2H), 5.35 (s, 2H).

2.2.3. Synthesis of 4,4'-dinitro-4''-*N*-carbazolyltriphenylamine (3)

A mixture of 9.041 g (0.035 mol) of compound 2, 10.12 g (0.072 mol) of 4-fluoronitrobenzene, 7.245 g (0.0525 mol) of anhydrous potassium carbonate, 80 mL of dry *N,N*-dimethylformamide (DMF) was in a 250-mL, three-necked, round-bottomed flask equipped with a mechanical stirrer, a Dean–Stark strap, a reflux condenser and a nitrogen purge. The mixture was refluxed at 150 °C with stirring for 10 h under a nitrogen atmosphere. After being poured into water (500 mL), the red precipitate was collected by filtration and dried under vacuum. The crude product was crystallized from DMF to obtain red crystals. Yield, 70 %, T_m : 282 °C. IR (KBr): 1578, 1311 cm^{-1} (NO_2 stretch). ^1H NMR (500 MHz, $\text{DMSO}-d_6$, δ , ppm): 8.50 (d, 4H), 8.03 (d, 2H), 7.87 (d, 2H), 7.72 (m, 8H), 7.57 (m, 4H).

2.2.4. Synthesis of 4,4'-diamino-4''-*N*-carbazolyltriphenylamine (4)

In a 250 mL round-bottom flask equipped with a stirring bar, a mixture of 5.5 g of dinitro compound 3, 0.05 g of 10 % Pd/C, 5 mL of hydrazine monohydrate, and 100 mL of ethanol was heated at reflux for 10 h and cooled to room temperature. Pd/C was removed by filtration through Celite. The crude product was crystallized from ethanol under nitrogen and dried in vacuum at 70 °C. Yield, 90 %, T_m : 110–112 °C. IR (KBr): 3467, 3455 cm^{-1} (NH_2 stretch). ^1H NMR (500 MHz, $\text{DMSO}-d_6$, δ , ppm): 8.17 (d, 2H), 7.39 (t, 2H), 7.28 (d, 2H), 7.22 (m, 4H), 6.95 (d, 4H), 6.76 (d, 2H), 6.58 (d, 4H), 5.01 (s, 4H, $-\text{NH}_2$). ^{13}C NMR (126 MHz, $\text{DMSO}-d_6$, δ , ppm): 149.68, 146.67, 141.18,

135.80, 128.38, 127.74, 126.47, 126.42, 122.77, 120.83, 119.97, 116.81, 115.40, 110.14.

2.2.5. Synthesis of 4,4'-bis(trimellitimido)-4''-*N*-carbazolyltriphenylamine (5)

A flask was charged with 4.4 g (0.01 mol) of 4,4'-diamino-4''-*N*-carbazolyltriphenylamine (4), 3.84 g (0.02 mol) of trimellitic anhydride, and 60 ml of glacial acetic acid. The heterogeneous mixture was stirred for 1 h and then refluxed at 140 °C for 12 h. The reaction mixture was cooled to precipitate a yellowish brown powder which was rinsed with methanol to remove acetic acid. The product was filtered several times with methanol and dried in vacuum at 50 °C. Yield, 87 %, T_m : 274–276 °C. IR (KBr): 3500–2400 cm^{-1} (OH stretch); 1780, 1722 cm^{-1} (imide C=O). ^1H NMR (500 MHz, $\text{DMSO}-d_6$, δ , ppm): 13.7(s, 2H, $-\text{COOH}$), 8.42 (dd, 2H), 8.32 (s, 2H), 8.25 (d, 2H), 8.10 (d, 2H), 7.62 (d, 2H), 7.46 (m, 8H), 7.40 (d, 2H), 7.35 (d, 4H), 7.29 (t, 2H). ^{13}C NMR (126 MHz, $\text{DMSO}-d_6$, δ , ppm): 166.9, 166.3, 147.0, 146.3, 140.7, 135.9, 135.9, 135.4, 132.6, 132.4, 129.1, 128.6, 127.3, 126.7, 125.8, 124.5, 124.3, 123.8, 123.1, 121.0, 120.5, 110.3.

2.2.6. Polymer synthesis

Utilizing compound 5 as diimide-diacid monomer, four kinds of PAIs were synthesized by polycondensation with diamine monomers ODA (6a), APB (6b), 6FAPB (6c) and 4,4'-diamino-4''-*N*-carbazolyltriphenylamine (6d), respectively. The resulting PAIs were abbreviated to 7a–7d successively.

In a typical experiment, PAI-7a, which derived from diimide-diacid 5 and ODA (6a) was prepared as follows: a mixture of 0.7888 g (1 mmol) of the diimide-diacid monomer 5, 0.2002 g of ODA (6a), 0.15 g of anhydrous calcium chloride, 1.2 ml of triphenyl phosphite (TPP), 0.4 ml of pyridine, and 3.5 ml of NMP was heated with stirring at 120 °C for 3 h. The resulting polymer solution was poured slowly into 200 ml of stirred methanol giving rise to a tough, fiber-like precipitate that was collected by filtration, and washed thoroughly with hot water and methanol and dried.

A solution of the polymer was obtained by dissolving about 1.0 g PAI sample in 10 ml of NMP. The homogeneous solution was poured onto a 6 cm glass Petri dish, which was placed in a 90 °C overnight for the slow release of the solvent, and then the film was stripped from the glass substrate and further dried in vacuum at 180 °C for 5 h. The thickness of the films were about 70–80 μm and the films were used for X-ray diffraction measurements, solubility tests and thermal analyses. Other PAIs were synthesized in an analogous procedure. The characterization of the target PAIs are listed as follows.

PAI-7a: IR (KBr, cm^{-1}): 3349 cm^{-1} (N–H stretching), 1779, 1723 cm^{-1} (C=O stretching), 1374 (C–N stretching). Anal. Calcd for $(\text{C}_{60}\text{H}_{36}\text{N}_6\text{O}_7)_n$: C, 75.62%, H, 3.81%, N, 8.82%. Found: C, 74.12%, H, 3.54%, N, 8.55%. ^1H NMR (500 MHz, $\text{DMSO}-d_6$, δ , ppm): 10.66 (s, 2H, NH-CO), 8.57 (s, 2H), 8.47 (d, 2H), 8.25 (d, 2H), 8.14 (d, 2H), 7.85 (d, 4H), 7.63 (d, 2H), 7.52 (d, 4H), 7.47(s, 4H), 7.40 (dd, 6H), 7.30 (s, 2H), 7.08 (d,4H).

PAI-7b: IR (KBr, cm^{-1}): 3349 cm^{-1} (N–H stretching), 1779, 1723 cm^{-1} (C=O stretching), 1374 (C–N stretching). Anal. Calcd for $(\text{C}_{66}\text{H}_{40}\text{N}_6\text{O}_8)_n$: C, 75.85%, H, 3.86%, N, 8.04%. Found: C, 73.96%, H, 3.61%, N, 7.95%. ^1H NMR (500 MHz, DMSO- d_6 , d, ppm): 10.67 (s, 2H, NH-CO), 8.57 (s, 2H), 8.47 (d, 2H), 8.25 (d, 2H), 8.15 (d, 2H), 7.84 (d, 4H), 7.63 (d, 2H), 7.51 (d, 4H), 7.47 (s, 4H), 7.37 (dd, 6H), 7.30 (s, 2H), 7.07 (s, 8H).

PAI-7c: IR (KBr, cm^{-1}): 3350 cm^{-1} (N–H stretching), 1779, 1723 cm^{-1} (C=O stretching), 1379 (C–N stretching). Anal. Calcd for $(\text{C}_{68}\text{H}_{38}\text{F}_6\text{N}_6\text{O}_8)_n$: C, 69.15%, H, 3.24%, N, 7.12%. Found: C, 67.89%, H, 3.31%, N, 7.33%. ^1H NMR (500 MHz, DMSO- d_6 , d, ppm): 10.88 (s, 2H, NH-CO), 8.59 (s, 2H), 8.48 (d, 2H), 8.34 (d, 2H), 8.25 (d, 2H), 8.15 (d, 4H), 7.63 (d, 2H), 7.52 (d, 4H), 7.47 (s, 4H), 7.37 (dd, 6H), 7.30 (s, 2H), 7.18 (s, 2H), 7.14 (s, 4H).

PAI-7d: IR (KBr, cm^{-1}): 3349 cm^{-1} (N–H stretching), 1779, 1723 cm^{-1} (C=O stretching), 1373 (C–N stretching). Anal. Calcd for $(\text{C}_{78}\text{H}_{48}\text{N}_8\text{O}_6)_n$: C, 78.51%, H, 4.05%, N, 9.39%. Found: C, 77.07%, H, 4.13%, N, 9.72%. ^1H NMR (500 MHz, DMSO- d_6 , d, ppm): 10.69 (s, 2H, NH-CO), 8.58 (s, 2H), 8.49 (d, 2H), 8.26 (d, 4H), 8.15 (d, 4H), 8.01 (d, 2H), 7.88 (m, 4H), 7.51 (d, 2H), 7.47 (m, 4H), 7.38 (dd, 6H), 7.30 (s, 2H), 7.18 (s, 2H), 7.12 (s, 2H).

3. Results and discussion

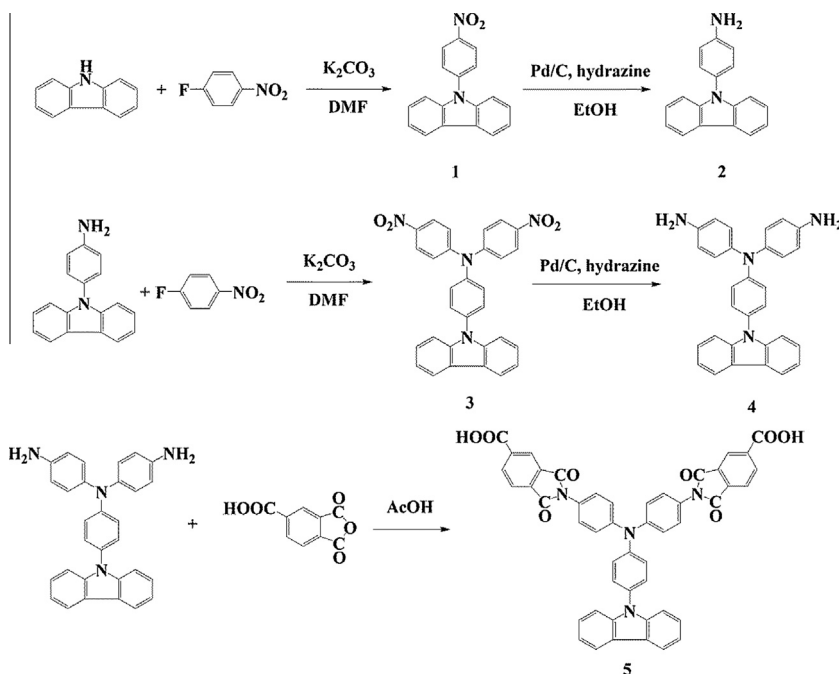
3.1. Monomer synthesis

The new diimide-diacid monomer 5 containing carbazole and triphenylamine groups was synthesized by the synthetic route outlined in Scheme 1. The targeted diimide-diacid 5 was prepared by the condensation of

diamine compound 4 with two molar equivalents of TMA in refluxing glacial acetic acid.

N-(4-Aminophenyl) carbazole 2 was prepared by the condensation of carbazole with 4-fluoronitrobenzene followed by hydrazine Pd/C catalytic reduction. The double-coupling reaction of the conjugate base of compound 2 with 4-fluorobenzonitrile produced dinitro compound 3, and diamine compound 4 underwent reduction with Pd/C catalyst in ethanol. The targeted diimide-diacid 5 was prepared by the condensation of 4 with two molar equivalents of TMA in refluxing glacial acetic acid. The synthetic route is shown in Scheme 1. Elemental analysis, IR, ^1H and ^{13}C NMR spectroscopic techniques were used to identify the structures of the intermediate compounds 1, 2, 3, 4 and the diimide-diacid monomer 5. The transformation of amino to carboxyl functional groups could be monitored by the change of IR spectra (Fig. 1). The IR spectrum of the diimide-diacid monomer 5 shows absorption bands at 3500–2400 cm^{-1} (OH stretching), 1780 cm^{-1} (imide, symmetric C=O stretching) and 1722 cm^{-1} (asymmetric imide C=O stretching).

Fig. 2 illustrates the H–H COSY spectra of diimide-diacid monomer 5. Assignments of each proton and carbon are also given in these figures, and agree well with the proposed molecular structure. In H–H COSY spectra, the correlated pairs of AB doublets at 7.62/7.40 ppm and 7.46/7.35 ppm can be easily assigned to the protons 5–8 on the triphenylamine core. The aromatic protons 10 appeared at the most downfield (8.42 ppm) owing to the strong electron-withdrawing effect of the C=O group as a doublet. Accordingly, the connected doublet signal at 8.10 ppm is assigned to the protons 9. The complicated resonances in the region of 7.50–7.46 ppm are assigned to the interconnected protons 3 (as a triplet), protons 4 (as a dou-



Scheme 1. Synthesis of monomer.

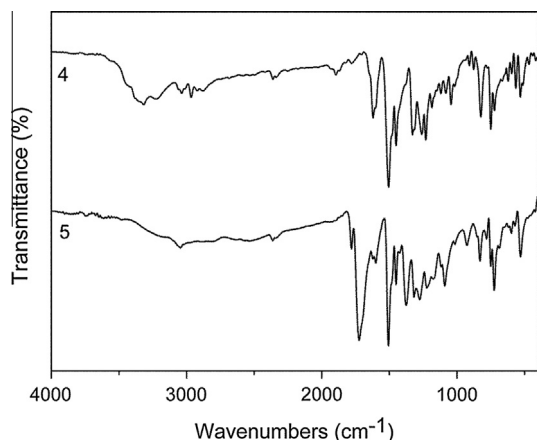


Fig. 1. FTIR spectra of diamine monomer 4 and diimide-diacid monomer 5.

blet) and protons 7 (as a doublet), in which the triplet of protons 3, doublet of protons 4 and the doublet of protons 7, is also connected with the triplet signal at 7.29 ppm arising from protons 2 and doublet signal at 7.35 ppm arising from protons 8. Fig. 3 shows the ^{13}C NMR spectra of diimide-diacid monomer 5, the carbonyl carbon atoms (C_o and C_v) appeared in the downfield (166.9 ppm) of the spectrum and the carbon atom (C_e) appeared in the upfield (110.3 ppm).

3.2. Polymer synthesis

According to the phosphorylation polyamidation technique first described by Yamazaki and co-workers [27], a

series of novel PAIs 7a–g were synthesized from the polycondensation reactions of diimide-dicarboxylic acid 5 with various aromatic diamines 6a–d by using triphenyl phosphite (TPP) and pyridine as condensing agents (Scheme 2). The polymerization proceeded homogeneously throughout the reaction and afforded clear, highly viscous polymer solution. All the PAIs precipitated in a tough, fiber-like form when the resulting polymer solutions were slowly poured under stirring into methanol.

As shown in Table 1, the inherent viscosities of the intermediate PAIs ranged from 0.78 dL/g to 0.96 dL/g. The weight-average molecular weight ($M_{\text{w,s}}$) and number-average molecular weights ($M_{\text{n,s}}$) were recorded in the ranges of 46,000–70,000 and 27,000–39,000, relative to polystyrene standards. The molecular weights of all the PAIs were sufficiently high to permit the casting of flexible and tough PAIs films.

The formation of PAIs was confirmed with elemental analysis and IR spectroscopy. As shown in Fig. 4, the IR spectra of these PAIs exhibited characteristic imide absorption bands at around 1779 cm^{-1} (imide carbonyl asymmetrical stretching), 1723 cm^{-1} (imide carbonyl symmetrical stretching), 1374 cm^{-1} (C–N stretching), together with some strong absorption bands in the region of $1100\text{--}1300\text{ cm}^{-1}$ due to the C–O and C–F multiple stretching. In addition to IR spectra, the elemental analysis results of these PAIs also generally agree with the calculated values for the proposed structures. The ^1H NMR spectra of PAI 4a are shown in Fig. 5. The amide group appeared in 10.66 ppm. The H_i close to the imide ring appeared at the farthest downfield region of the spectrum because of the resonance. The proton H_h shifted to a higher field because of the electron-donating property of amine group. The above results

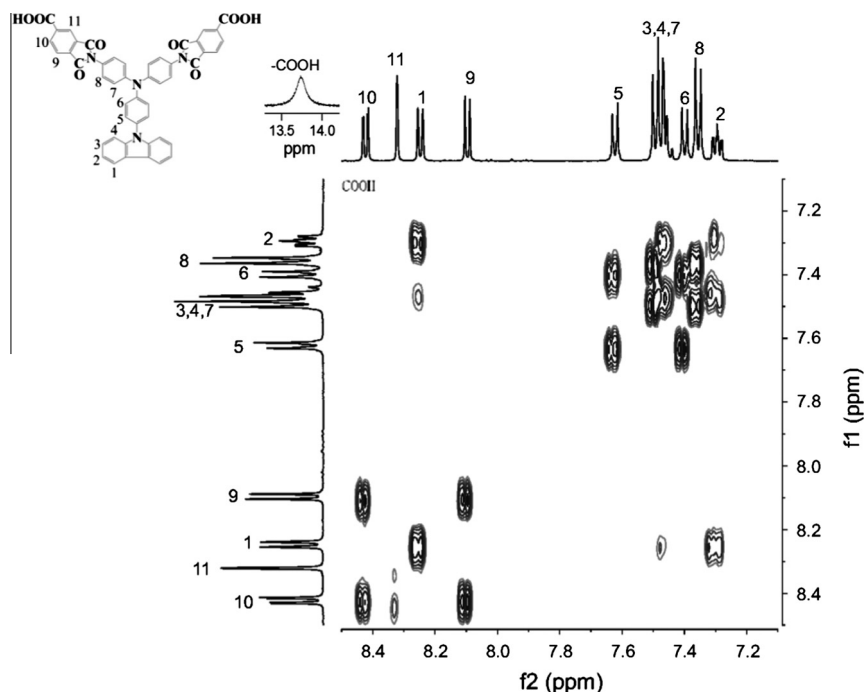


Fig. 2. H–H COSY spectra of diimide-diacid monomer 5 in $\text{DMSO-}d_6$.

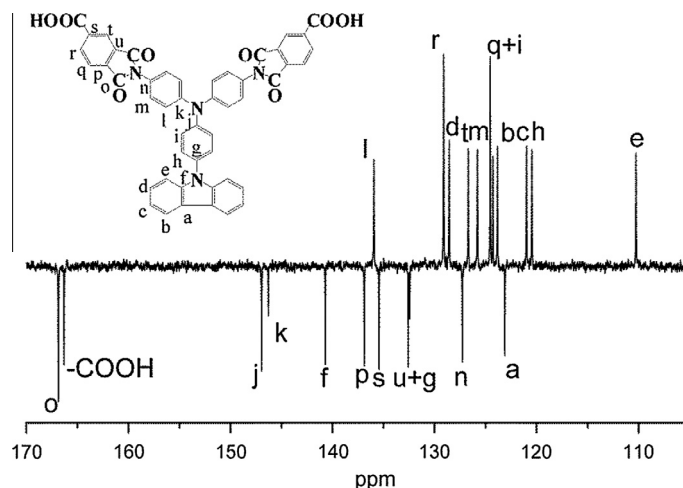
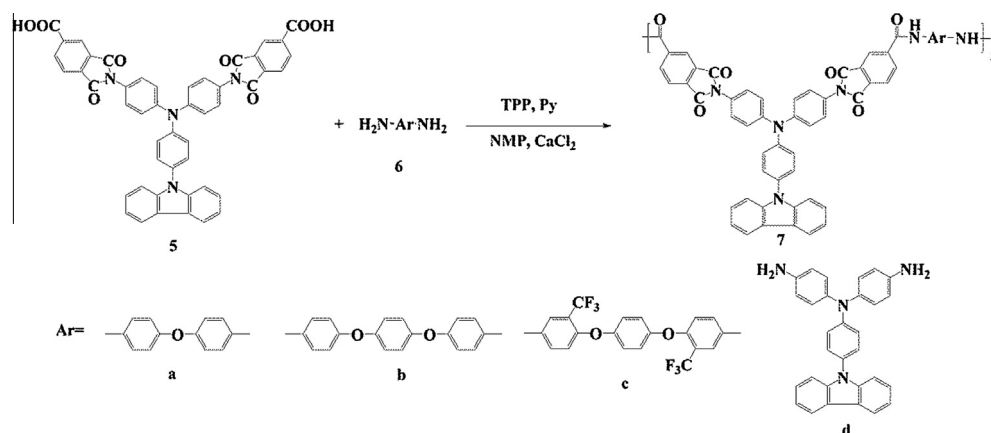


Fig. 3. ^{13}C NMR spectra of diimide-diacid monomer 5 in $\text{DMSO-}d_6$.



Scheme 2. Synthesis of the PAIs.

Table 1

Inherent viscosity, GPC data and solubility of the PAIs.

Polymer	η (dL/g) ^a	GPC data ^b			Solvents ^c						
		$M_w \times 10^4$	$M_n \times 10^4$	PDI	NMP	DMAc	DMF	DMSO	m-Cresol	THF	CHCl_3
PAI-7a	0.85	5.4	3.4	1.6	++	++	+	++	+	–	–
PAI-7b	0.92	6.2	3.9	1.6	++	++	+	+	+	–	–
PAI-7c	0.96	7.0	3.7	1.9	++	++	++	++	++	+	–
PAI-7d	0.78	4.6	2.7	1.7	++	++	++	++	++	±	–

++: Soluble at room temperature; +: soluble on heating; ±: partially soluble on heating.

^a Measured at a polymer concentration of 0.5 g/dL in NMP at 30 °C.

^b Relative to polystyrene standard, using DMF as the eluent.

^c Qualitative solubility was determined with as 10 mg of polymer in 1 mL of solvent.

demonstrate that the diimide-diacid monomer (5) hold a good polymerization activity to form PAIs.

WAXD experiments were conducted in an attempt to evaluate the morphological structure of our synthesized PAIs. As shown in Fig. 6, the curves of all the PAIs were broad and without obvious peak features, indicating their amorphous structure. Their amorphous properties could be attributed to the incorporation of packing-disruptive

triphenylamine and carbazole units along the polymer backbone, which resulted in a high steric hindrance for close packing, and thus reduced their crystallization tendency. The amorphous structure endowed the obtained PAIs with good solubility.

The solubility of synthesized PAIs was tested in a variety of organic solvents at 1.0% (w/v) and the results are summarized in Table 1. All the PAIs showed high solubility

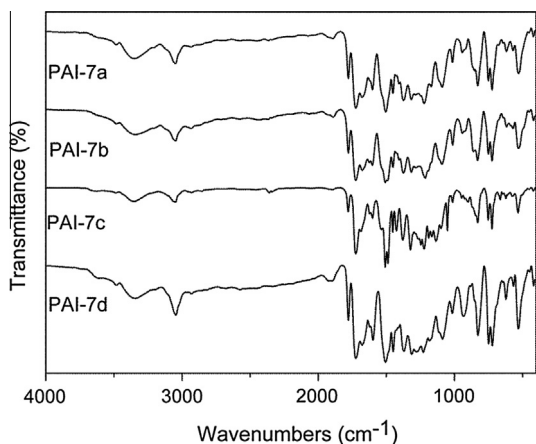


Fig. 4. FTIR spectra of the PAIs.

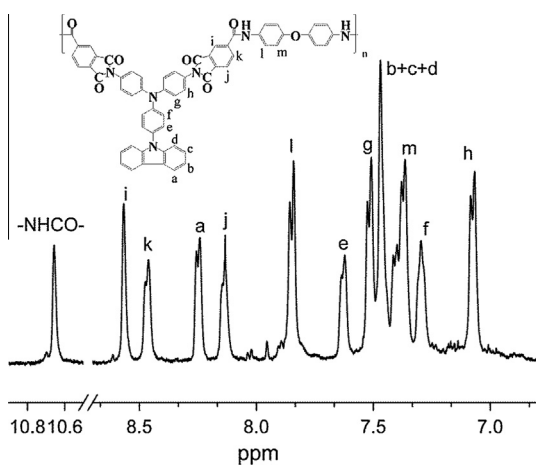


Fig. 5. ^1H NMR spectra of PAI-7a in DMSO- d_6 .

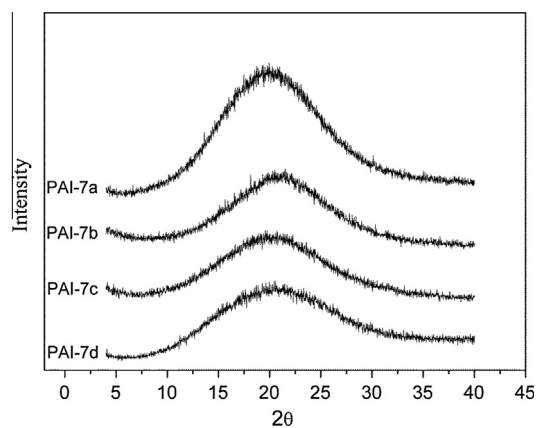


Fig. 6. Wide-angle X-ray diffractograms of the PAIs.

in aprotic polar solvents such as NMP, DMAc, DMF, DMSO and *m*-Cresol due to the introduction of propeller-shaped triphenylamine core and bulky pendent carbazole group

in the repeat unit. The excellent solubility makes these PAIs potential candidates for practical applications in spin- or dip-coating processes. Thus, all these PAIs can be readily processed from solution.

Flexible and tough films can be obtained via solvent casting. These films were subjected to tensile testing, and the results are given in Table 2. The tensile strengths, elongations to break, and initial moduli of these films were in the ranges of 76–85 MPa, 12–19% and 2.0–2.4 GPa, respectively.

3.3. Thermal properties of the PAIs

DSC was used to evaluate the thermal properties of the PAI films. The thermal behavior data of all the PAIs are also listed in Table 3. Generally, the decreasing order of T_g correlated with both molecular packing and chain conformation (chain rigidity and linearity) of the PAIs. The T_g values of these PAIs were in the range of 269–297 °C. The T_g value of PAI-7c is lower than PAI-7a because of the introduction of two flexible ether segments group in diamine monomer, which could increase the polymer chain mobility. Besides the trifluoromethyl groups could decrease the interchain interaction and chain packing density. These groups also lead to an internal plasticization in addition to the geometry and free volume factors.

Thermal stabilities of the PAIs were evaluated by TGA under nitrogen with a 5% weight loss and 10% weight loss for comparison. The results are summarized in Table 3. The decomposition temperatures at a 5% weight loss and 10% loss of PAIs were in the range of 526–561 °C and 565–580 °C, respectively. All the PAIs exhibited excellent thermal stability, and no obvious decomposition was observed below 500 °C. The amount of carbonized residue (char yield) of these polymers in nitrogen atmosphere was more than 65% at 800 °C. The high char yields of these PAIs could be ascribed to their high aromatic content. The outstanding thermal stability was also an advantage in various applications.

3.4. Electrochemical characteristics

The electrochemical properties of the PAIs were investigated by cyclic voltammetry (CV) conducted for the cast films on an ITO-coated glass substrate as working electrode (CH_3CN) in dry acetonitrile containing 0.1 M of TBAP as an electrolyte under nitrogen atmosphere. CV data for the PAIs are given in Table 4, and typical representative cyclic voltammogram of PAI-7a is shown in Fig. 7. The PAIs 7a–7d revealed two reversible redox couples at half-wave potential of 1.05–1.08 V ($E_{ox1\ 1/2}$) and 1.38–1.46 V ($E_{ox2\ 1/2}$), respectively, under an anodic sweep. The first electron removal of PAI-7a was assumed to occur at the nitrogen atom on the main chain triphenylamine unit, which was more electron-rich than the nitrogen atom on the pendent carbazolyl moiety at $E_{p,a} = 1.72$ V. Thus, the first stable cationic radical of PAI* should be formed by the first oxidation at the nitrogen atom of triphenylamine unit. The energy levels of the HOMO and LUMO of the investigated PAIs can be estimated from the oxidation onset (E_{onset}) or half-wave potentials ($E_{1/2}$), and the results

Table 2
Mechanical properties of PAIs.

Polymer	Tensile strength (MPa)	Elongation at break (%)	Initial modulus (GPa)
PAI-7a	85	14	2.4
PAI-7b	78	19	2.2
PAI-7c	76	18	2.2
PAI-7d	82	12	2.0

Table 3
Thermal properties of the PAIs.

Polymer	DSC		TGA	
	T_g^a (°C)	$T^b_{5\%}$ (°C)	$T^b_{10\%}$ (°C)	Char yield ^c (%)
PAI-7a	297	541	570	75
PAI-7b	277	550	578	71
PAI-7c	269	526	565	68
PAI-7d	275	561	580	70

^a Baseline shift in the second heating DSC traces, with a heating rate of 20 °C/min in nitrogen.

^b Temperature at 5% and 10% weight loss were recorded by TGA at a heating at 10 °C/min in nitrogen.

^c Residual weight (%) when heated to 800 °C.

are listed in Table 4. For example, the E_{onset} value for PAI-7a has been determined 0.92 eV. The external ferrocene/ferrocenium (Fc/Fc⁺) redox standard $E(\text{Fc}/\text{Fc}^+)$ was 0.48 V vs Ag/AgCl in CH₃CN. Assuming that the HOMO energy level of the Fc/Fc⁺ standard is 4.80 eV with respect to the zero vacuum level, the HOMO energy level of PAI-7a has been evaluated to be 5.24 eV. The high-lying HOMO energy level and reversible electrochemical oxidation of these PAIs suggest that they have potential for use as hole injection and transport materials in the organic light-emitting devices.

3.5. Electrochromic characteristics

Electrochromism of the PAIs thin films was determined by optically transparent thin-layer electrode (OTTE) coupled with a UV–vis spectroscopy. The electrode preparations and solution conditions were identical to those used in cyclic voltammetry. The typical electrochromic absorption spectrum of PAI-7a is shown in Fig. 8. When the applied potentials increased positively from 0 V to 1.68 V, the peak of characteristic absorbance at 322 nm for PAI-7a decreased gradually while three new bands grew up at 421 nm and 776 nm. The film of PAI-7a

Table 4
Electrochemical properties of the PAIs.

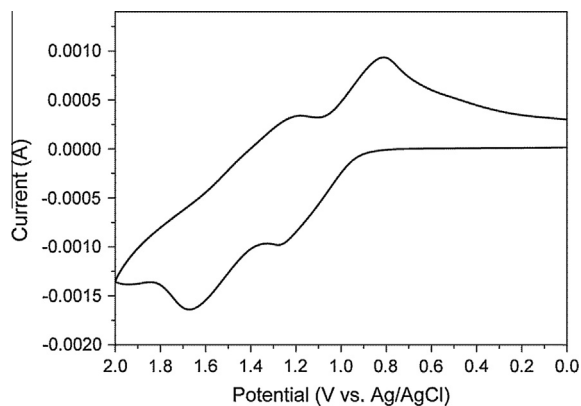
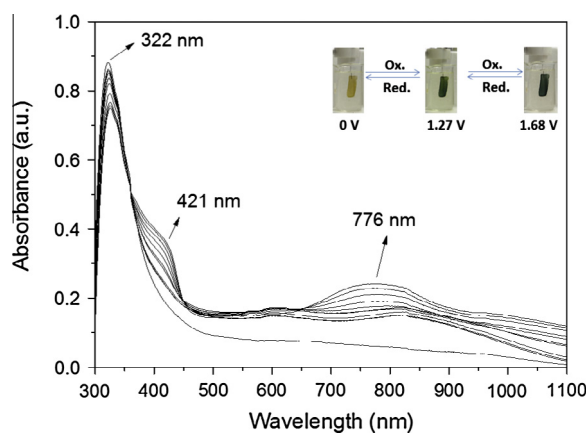
Index	Thin film (λ/nm)		Oxidation potential ^a (V)			E_g^b (eV)	HOMO ^c (eV)	LUMO ^d (eV)
	Abs. max	Abs. onset	E_{onset}	$E_{1/2}^{\text{ox}1}$	$E_{1/2}^{\text{ox}2}$			
PAI-7a	322	421	0.92	1.05	1.43	2.58	5.24	2.66
PAI-7b	310	415	0.90	1.06	1.46	2.60	5.22	2.62
PAI-7c	318	411	0.95	1.08	1.44	2.61	5.27	2.66
PAI-7d	315	409	0.96	1.06	1.38	2.59	5.28	2.69

^a Oxidation half-wave potentials from cyclic voltammograms.

^b The data were calculated by the equation: $E_g = 1240/\lambda_{\text{onset}}$ of polymer film.

^c The HOMO energy levels were calculated from cyclic voltammetry and were referenced to ferrocene (4.8 eV).

^d LUMO = HOMO – E_g .

**Fig. 7.** Repeated CV of PAI-7a films on the ITO-coated glass substrate in 0.1 M Bu₄NClO₄ at a scan rate of 100 mV/s.**Fig. 8.** Spectroelectrochemistry of the cast film of PAI-7a on the ITO-coated glass substrate in 0.1 M Bu₄NClO₄ at various applied potentials.

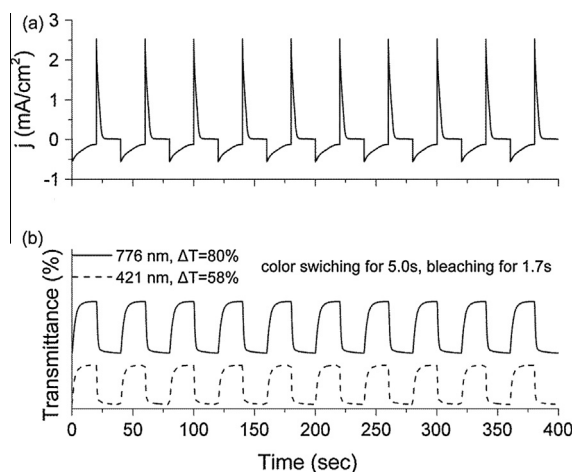


Fig. 9. (a) Current densities during switching studies. (b) Optical transmittance change monitored at 412 nm and 763 nm for PAI-7a thin film on the ITO-coated glass substrate in 0.1 M $\text{Bu}_4\text{NClO}_4/\text{CH}_3\text{CN}$ solution.

switches from a transmissive neutral state (pale yellowish) to a high absorbing semioxidized state (green) and fully oxidized state (dark blue).

Optical switching studies were examined for probing changes in transmittance while repeatedly stepping the potential between neutral and oxidized states. The PAI film was cast onto an ITO-coated glass slides in the same manner as described earlier. We extracted the electrochromic parameters of the PAI-7a film by analysis of transmittance change decrement or increment of the absorption at 421 nm and 776 nm with respect to time while the potential was switched stepwise between the neutral (0 V) and the oxidized state at +1.27 V with a residence time of 40 s. During this measurement, the percent transmittance (%T) values at the indicated wavelengths were measured using a UV-vis-NIR spectrophotometer. The results for the first 10 cycles are shown in Fig. 9. The optical contrast measured according to the difference between %T of PAI-7a at 0 V and 1.27 V was found to be 58% and 80% at 421 and 776 nm, respectively. The PAI-7a requires 5.0 s at 1.27 V for switching the absorbance at 776 nm, and 1.7 s for bleaching. After over hundreds of cyclic scans between 0 V and 1.27 V, the PAI-7a film still exhibited good electrochemical and electrochromic reversibility.

The electrochromic coloration efficiency (CE; η) can be calculated via optical density using the following equation:

$$\eta = \Delta OD / Q \quad (1)$$

where ΔOD is the optical absorbance change and Q (mC/cm^2) is the injected/ejected charge during a redox step. Based on this equation, the CE of PAI-7a was found to be $205 \text{ cm}^2/\text{C}$, which was higher than that of many conjugated polymers.

4. Conclusions

A series of new redox-active PAIs (7a–d) bearing pendent triphenylamine and carbazole groups have been prepared from 4,4'-bis(trimellitimidio)-4''-N-carbazolytri-

phenylamine (5) with various aromatic diamines (6a–d). The incorporation of triphenylamine and carbazole substituents to the polymer main chain, not only facilitates the electrochromic behaviors by adjusting the oxidation potentials, but also enhances the solubility. Besides high T_g and T_d values and good thermal stability, the PAIs also revealed stable electrochromic properties, changing color from original pale yellowish neutral form to the green and then to dark blue oxidized forms. The PAI-7a film exhibited high coloration efficiency, high optical contrast ratio, long-term redox and electrochromic reversibility. Thus, these PAIs might have optoelectronic applications such as new hole-transporting and electrochromic materials because of their proper HOMO values and stable electrochromic behavior.

Acknowledgements

We thank the National Science Foundation of China (51203172) and Liaoning Province Doctor Startup Fund (20121067) for the financial support.

References

- [1] P.M.S. Monk, R.J. Mortimer, D.R. Rosseinsky, *Electrochromism and Electrochromic Devices*, Cambridge University Press, Cambridge, UK, 2007.
- [2] R.D. Rauh, *Electrochim. Acta* 44 (1999) 3165.
- [3] D.R. Rosseinsky, R. Mortimer, *J. Adv. Mater.* 13 (2001) 783.
- [4] H.W. Heuer, R. Wehrmann, S. Kirchmeyer, *Adv. Funct. Mater.* 12 (2002) 89.
- [5] R.J. Mortimer, A.L. Dyer, J.R. Reynolds, *Displays* 27 (2006) 2.
- [6] G. Sonmez, H.B. Sonmez, *J. Mater. Chem.* 16 (2006) 2473.
- [7] P. Andersson, R. Forchheimer, P. Tehrani, M. Berggren, *Adv. Funct. Mater.* 17 (2007) 3074.
- [8] R. Baetens, B.P. Jelle, A. Gustavsen, *Sol. Energy Mater. Sol. Cells* 94 (2010) 87.
- [9] S. Beaupré, A.-C. Breton, J. Dumas, M. Leclerc, *Chem. Mater.* 21 (2009) 1504.
- [10] P.M. Beaujuge, J.R. Reynolds, *Chem. Rev.* 110 (2010) 268.
- [11] (a) M.A. Invernale, Y. Ding, D.M.D. Mamangun, M.S. Yavuz, G.A. Sotzing, *Adv. Mater.* 22 (2010) 1379; (b) P.M. Beaujuge, S. Ellinger, J.R. Reynolds, *Nat. Mater.* 7 (2008) 795–799; (c) A. Balan, D. Baran, G. Gunbas, A. Durmus, F. Ozyurt, L. Toppare, *Chem. Commun.* 21 (2009) 6768; (d) M. İcli, M. Pamuk, F. Algi, A.M. Önal, A. Cihaner, *Chem. Mater.* 22 (2010) 4034.
- [12] D.A. Tomalia, A.M. Naylor, W.A. Goddard, *Angew. Chem. Int. Ed. Engl.* 29 (1990) 138.
- [13] D. Wilson, H.D. Stenzenberger, P.M. Hergenrother, *Polyimides*, Chapman and Hall, New York, 1990.
- [14] M.K. Ghosh, K.L. Mittal, *Polyimides Fundamentals and Applications*, Marcel Dekker, New York, 1996.
- [15] K. Xie, J.G. Liu, H.W. Zhou, S.Y. Zhang, M.H. He, S.Y. Yang, *Polymer* 42 (2001) 7276.
- [16] M. Hasegawa, K. Horie, *Prog. Polym. Sci.* 26 (2001) 259.
- [17] (a) Y. Liu, Y.H. Zhang, S.W. Guan, Z.H. Jiang, *Polymer* 49 (2008) 5439; (b) Y. Liu, Y.H. Zhang, S.W. Guan, H.B. Zhang, X.G. Yue, Z.H. Jiang, *J. Polym. Sci. Part A: Polym. Chem.* 47 (2009) 6269; (c) Y. Liu, Y. Xing, Y.H. Zhang, S.W. Guan, H.B. Zhang, Y. Wang, Y.P. Wang, Z.H. Jiang, *J. Polym. Sci. Part A: Polym. Chem.* 48 (2010) 3281; (d) Y. Liu, H.Y. Yao, Y.H. Zhang, H.B. Zhang, J.X. Mu, Z.H. Jiang, S.W. Guan, *J. Appl. Polym. Sci.* 127 (2013) 1834.
- [18] H. Behniafar, A. Banihashemi, *Eur. Polym. J.* 40 (2004) 1409.
- [19] A. Sarkar, P.N. Honkhambe, C.V. Avadhani, P.P. Wadgaonkar, *Eur. Polym. J.* 43 (2007) 3646.
- [20] (a) G.S. Liou, H.W. Chen, H.J. Yen, *Macromol. Chem. Phys.* 207 (2006) 1589; (b) C.W. Chang, G.S. Liou, *Org. Electron.* 8 (2007) 662; (c) L.T. Huang, H.J. Yen, J.H. Wu, G.S. Liou, *Org. Electron.* 13 (2012) 840.

- [21] (a) J.A. Mikroyannidis, K.M. Gibbons, A.P. Kulkarni, S.A. Jenekhe, *Macromolecules* 41 (2008) 663;
(b) M.H. Park, J.O. Huh, Y. Do, M.H. Lee, *J. Polym. Sci. Part A: Polym. Chem.* 46 (2008) 5816;
(c) J.H. Park, C. Yun, M.H. Park, Y. Do, S. Yoo, M.H. Lee, *Macromolecules* 42 (2009) 6840;
(d) B.-Y. Hsieh, Y. Chen, *J. Polym. Sci. Part A: Polym. Chem.* 47 (2009) 1553;
(e) G. Nursalim, Y. Chen, *Polymer* 51 (2010) 3187;
(f) Z.M. Wang, X.H. Song, L.L. Ma, Y. Feng, C. Gu, X.J. Zhang, P. Lu, Y.G. Ma, *New J. Chem.* (2013) 2440.
- [22] (a) M.K. Leung, M.Y. Chou, Y.O. Su, C.L. Chiang, H.L. Chen, C.F. Yang, C.C. Yang, C.C. Lin, H.T. Chen, *Org. Lett.* 5 (2003) 839;
(b) S. Beaupré, J. Dumas, M. Leclerc, *Chem. Mater.* 18 (2006) 4011;
(c) L. Otero, L. Sereno, F. Fungo, Y.-L. Liao, C.-Y. Lin, K.-T. Wong, *Chem. Mater.* 18 (2006) 3495;
(d) J. Natera, L. Otero, L. Sereno, F. Fungo, N.-S. Wang, Y.-M. Tsai, T.-Y. Hwu, K.-T. Wong, *Macromolecules* 40 (2007) 4456.
- [23] (a) J.P. Chen, A. Natansohn, *Macromolecules* 32 (1999) 3171;
(b) J.-F. Morin, M. Leclerc, D. Adès, A. Siove, *Macromol. Rapid Commun.* 26 (2005) 761.
- [24] L. Hagopian, G. Kohler, R.I. Walter, *J. Phys. Chem.* 71 (1967) 2290.
- [25] A. Ito, H. Ino, K. Tanaka, K. Kanemoto, T. Kato, *J. Org. Chem.* 67 (2002) 491.
- [26] R. Gujadhur, D. Venkataraman, J.T. Kintigh, *Tetrahedron Lett.* 42 (2001) 4791.
- [27] (a) N. Yamazaki, F. Higashi, J. Kawabata, *J. Polym. Sci. Polym. Chem. Ed.* 12 (1974) 2149;
(b) N. Yamazaki, M. Matsumoto, F. Higashi, *J. Polym. Sci. Polym. Chem. Ed.* 13 (1975) 1371.